CERN 68-22
Intersecting Storage
Rings Division
4 June, 1968

ORGANISATION EUROPÉENNE POUR LA RECHERCHE NUCLÉAIRE
CERN EUROPEAN ORGANIZATION FOR NUCLEAR RESEARCH

BEAM STACKING WITH SUPPRESSED BUCKETS IN THE ISR

A.G. Ruggiero

G E N E V A
1968

Genève - Service d'Information scientifique - K/0694 - 1100 - juillet 1968

SUMMARY

The process of accumulating a beam in the CERN Intersecting Storage Rings (ISR) by radio-frequency stacking with suppressed buckets at $\Gamma = 0.50$ and at $\Gamma = 0.84$ was investigated on a computer.

The stacking efficiency was calculated for several values of the number of the suppressed buckets. The results show that within the statistical error, the stacking efficiency does not depend on the number of suppressed buckets provided one always injects such a number of pulses that the total numbers of stacked buckets are equal.

SOMMAIRE

Le procédé d'accumulation des faisceaux dans les Anneaux de Stockage du CERN (ISR) par Haute Fréquence avec suppression d'une certaine quantité de zones de stabilité a été étudié sur la calculatrice pour $\Gamma(= \sin \phi_s) = 0.50$ et 0.84.

L'efficacité du procédé d'accumulation a été calculé en fonction du nombre n de zones de stabilité éliminées.

Les résultats montrent que, à part les erreurs statistiques, l'efficacité ne change pas avec n si le nombre des impulsions accumulées dans les différents cas donne toujours la même quantité de particules stockées.

CONTENTS

1. Introduction

It is known that an RF bucket occupies the same amount of synchrotron phase space, whether it is empty or filled by the injected beam (in a circular accelerator). Hence, with the circumference ratio between the ISR and the PS the stacked current would be reduced to 2/3 of the possible maximum if the buckets left empty after the injection of one PS pulse were permitted to enter the stack. To avoid this drawback, A. Schoch proposed to suppress the empty buckets by switching off the RF when they pass the RF cavities. The idea has been exposed by W. Schnell in Refs.(1) and (2).

The first numerical investigation of stacking with missing buckets was carried out, using the algorithm exposed below (Ref.(3)). It was applied to a stacking experiment in CESAR where the computer results could be compared to the results of an actual experiment (Ref.(4)). The comparison is shown in Fig. 1 where the full lines represent the computer results. One can see that within the statistical error there was no difference in the efficiency between the normal stacking experiment and that of the missing bucket experiment provided that the equal numbers of full buckets were injected. This preliminary calculation was repeated for several other values of the ratio of the number of the suppressed buckets n to the RF harmonic number h, with the parameters of the ISR radio-frequency system in order to check whether or no the stacking process depends on the characteristics of the storage rings.

As mentioned in the summary, we investigated stacking at $\Gamma = 0.50$ and at $\Gamma = 0.84$ each with the following series of cases:

TABLE I

Case	No. of suppressed buckets, n	h
1	0	30
2	10	30
3	20	30
4	25	30

The case No. 1 is the normal stacking in which 20 ISR buckets are filled by the 20 PS bunches and 10 ISR buckets are left empty. The drawbacks of this scheme have already been explained. In case 2, the 10 empty buckets were suppressed. Cases Nos. 3 and 4 with 20 and 25 suppressed buckets respectively, were investigated to take into account the possibility of two or four turn injection into the ISR (Ref.[5]).

2. Algorithm for a stacking cycle

For the sake of convenience and also in order to define the notation which will be used later on, there follows a short description of the method used in this study. It has been suggested and used by D.A. Swenson (Ref.[6]) in 1961. Readers who wish to know more details of the method and of the present computer programmes based on it should refer to Ref.[7]. Further applications of the same method are given in Ref.[8] and [3].

The motion of a particle in a circular accelerator with RF cavities can be described in the plane (E,ϕ), where E is the total energy and ϕ the phase relative to one of the cavities(*). The radial extension of the vacuum chamber which can be occupied by particles corresponds in the (E,ϕ) plane to an energy interval with a lower boundary E_o, the injection value, and an upper boundary E_f. The stacking region is defined as the energy interval from E_1 to E_f, where $E_1 \geq E_o$.

The stacking region is subdivided into N_h channels of width ΔE. We now consider N_p particles with energy E and phase ϕ uniformly distributed in the reference channel N_r taking channels to be numbered from the bottom to the top.

We move m buckets up from the lowest level, E_o (m = h in the normal case and m = h-n in the case where n buckets are suppressed). The energy distribution of the particles will be modified during the time when the moving buckets traverse the stacking region.

(*) Here and in the following ϕ is normalized in such a way that the period (0.2π) contains exactly h buckets.

A first computer programme, ASTACK, traces the history of the N_p particles initially distributed inside the channel No. N_r, as they circulate and change energy by traversing the radio-frequency cavities. The output of this programme consists of the phase ϕ_i and the energy E_i of each particle at different times t_i at which the centre of the moving buckets crosses the centre E_i of the i^{th} channel, ($i = 1,2, \ldots, N_h$).

The results of the ASTACK programme are transferred by tape to the BSTACK programme which collects the energies of the N_p particles at each time t_i and forms the histogram V_i. The term "histogram" will be used only for the energy spectrum after one stacking cycle of a sample of particles initially within a single channel. There will be N_h histograms with serial numbers corresponding to the number of the channel in which the centre of the bucket was at the time t_i.

The sequence of the histograms V_i in the time from $i = 1$ to $i = N_h$ shows how the energy distribution of the particles is changing during a cycle.

The following assumptions are made:

i) That the energy distribution of the particles at the time t_i is adequately represented by the histogram V_i.

ii) Also that the histograms obtained for a sample of particles initially within the channel No. N_r after one stacking cycle, depend only on the difference of the energy of that channel and the energy E_i which the bucket was crossing (Ref.[6]).

iii) According to Ref.[8] all particles will have the same phase and be placed at equidistant intervals in energy, since a uniform distribution in energy also yields an almost uniform distribution in the Hamiltonian.

In order to reproduce initially the nearest uniform distribution in the Hamiltonian, it is required that the energy range covered, corresponding to the width of ΔE of a channel, is of the same order of magnitude as the distance in energy between an integer number ($\zeta + 1$) of adjacent separatrices, this distance being evaluated at the initial phase of the N_p particles.

3. Build-up of the stack: The stacking matrix

We assume that there is no interaction between the particles in a stacked beam. Thus all possible stack shapes can be investigated by linearly superimposing the effects of the moving buckets on the sample of particles.

A third programme, CSTACK, constructs a matrix A in which the histogram V_i, normalized to unity, appears as the i^{th} column in such a way that the elements of the principal diagonal are those contained in the reference channel No. N_r.

In Refs.(6)(7) and (8) it is shown that the change in the energy spectrum during the $(N + 1)^{th}$ cycle is described by a multiplication of the matrix A with a column vector V_N representing the energy spectrum of the particles after N cycles.

In order to take into account the effect of the particles brought up in the last buckets one has to add a column vector V_B. Thus the energy distribution after N + 1 cycles is represented by the vector:

$$V_{N+1} = AV_N + V_B \qquad (3.1)$$

At the first pulse, the vector V_o is filled with zeros.

Since the histograms which form the stacking matrix A are obtained by releasing the buckets always at the same final energy E_{N_h}, the iteration (3.1) can be applied immediately to a stacking process "at the top".

When stacking "at the bottom", the already stacked beam is never passed by subsequent buckets, because the buckets stop δE lower than the previous cycle. This can be simulated by shifting the beam up by δE between cycles. A reasonable choice for δE is given by analytical theory. It shows that in the normal case δE is the area of a bucket divided by 2π. In the case where n buckets are suppressed, we assume the displacement to be reduced by the factor (h-n)/h.

Before performing the product (3.1), the programme shifts up the vector V_N by Q channels. Obviously, Q should be an integer and this imposes a condition on the choice of the width ΔE of the channels in such a way that

$$\delta E = Q \, \Delta E \, .$$

If we call λ the ratio between the bucket area and the area of a channel, in the normal case, we have to take $Q = \lambda$ and in the case where n buckets are suppressed

$$Q = \frac{h-n}{h} \lambda \, . \qquad (3.2)$$

The number of stacking cycles is limited by the fact that an ideal stacking process, where the buckets are just deposited side by side, yields a stack of width $N\lambda$ channels after N cycles. Therefore, since the available number of channels is N_h, the results are expected to be wrong when the number of cycles is about N_h/λ for a matrix with N_h columns.

To overcome the difficulties of the finite storage size we use the following procedure.

As is shown in Ref.[8] the shape and the energy variance of the histograms do not change significantly when the moving buckets are either well above or well below the reference channel. Thus, one can assume that the first few histograms are identical within statistical errors; the same is also true for the last few histograms.

Making use of this fact, we construct an "expanded matrix" by copying the left most column towards the left of the actual matrix A and shifting it up by one place, and by copying the right most column towards the right and shifting it down by one place. This operation is repeated until the number of columns of the expanded matrix A is equal to the number of rows of the factor V_N before evaluating the product (3.1).

4. The stacking efficiency

In an ideal case a single pulse should occupy in the stacking region an interval of energy equivalent to Q times a channel, where Q is given by (3.2), thus after N cycles all the particles are collected in an interval of width QN channels. Therefore, for stacking at the top we evaluate the sum S_N of the contents in the channels between N_r and $N_r + QN - 1$ inclusive.

The stacking efficiency η_N is the ratio of the contents S_N in the real case to those in the ideal case. If each vector V_N is normalized to α (generally $\alpha = 1$ or Q or λ), the more general case in which n buckets are suppressed gives

$$\eta_N = \frac{S_N}{\alpha N} \qquad (4.1)$$

For stacking at the bottom the sum S_N is evaluated between the channels N_r and $N_r - QN + 1$ inclusive.

5. The match of the computer problem to the ISR problem

Because it is not "a priori" excluded that the efficiency of a stacking process depends on the actual parameters of the storage device, we would like them to be as close as possible to the ISR parameters.

The computer time required to process a particle in the programme ASTACK is given by the number N of revolutions of the particle during one cycle (see Ref.(7)).

Assuming that the cavities of the ISR are equivalent to a single cavity, we compute N and the time t_c needed to process a particle using the CDC 6400 in CERN for the cases shown in Table 1. N and t_c are listed in Table 2:

TABLE 2

Γ	0.50		0.84	
n = 0	$N = 1.4 \times 10^6$	t_c = 7'	$N = 4.0 \times 10^5$	t_c = 2'
10	9.0×10^6	45'	8.5×10^6	45'
20	9.0×10^6	45'	8.5×10^6	45'
25	1.7×10^7	85'	1.7×10^7	85'

To process 60 particles for all the 8 cases listed in Table 1 would require about 360 hours machine time!

To reduce the computer time we abandoned the complete matching and scaled appropriately the ratio Δ of the revolution frequency f to the phase oscillation frequency ν_ϕ of a particle in the proximity of the stable point. In the case of a single cavity the following relation holds for Δ

$$V = \frac{2\pi}{\cos(h\phi_s)} \frac{f^2}{h(f\frac{df}{dE})} \frac{1}{\Delta^2}$$

where V is the voltage across the cavity and ϕ_s is the synchronous value of the phase.

The actual values of Δ in the ISR are

$$\Delta = 86{,}000 \quad \text{for} \quad \Gamma = 0.50$$
$$24{,}000 \quad \text{for} \quad \Gamma = 0.84$$

We took in our computation $\Delta = 1000$.

Furthermore, we assumed that the computer problem simulates the actual problem when the trajectories of the particles computed in the first case correspond exactly to the theoretical trajectories of the second case in the synchrotron space phase (W,ϕ), and where W is the canonical variable

$$W = \frac{1}{2\pi} \int^{E} \frac{dE}{f(E)} \cdot \qquad (5.2)$$

As shown in Ref.[7], the matching of the trajectories can be obtained by matching exactly all the parameters of the storage ring except the energy E and the revolution frequency f which can be scaled by a suitably chosen α.

$$\alpha = 1/86 \quad \text{for} \quad \Gamma = 0.50$$
$$\alpha = 1/24 \quad \text{for} \quad \Gamma = 0.84$$

The values of N and t_c corresponding to this new situation are listed in Table 3.

TABLE 3

Γ	0.50		0.84	
n = 0	$N = 1.7 \times 10^4$	t_c = 5"	$N = 1.7 \times 10^4$	t_c = 5"
10	1.0×10^5	30"	3.5×10^5	1'45"
20	1.0×10^5	30"	3.5×10^5	1'45"
25	2.0×10^5	1'	7.0×10^5	3'30"

The total time needed to process 60 particles for all the 8 cases is thus reduced to about 10 hours, which is still fairly long.

Another method which reduces the computer time even more, is given below.

6. A method to reduce the computer time

As mentioned above the most important change of the energy distribution of the sample of particles initially located in channel No. N_r occurs when the buckets are in the proximity of that channel. In particular, when the buckets are far below the reference channel the distribution is unchanged.

We assume that the energy distribution of the particles remains unchanged from the beginning up to the time t_1 at which the buckets cross the first channel.

Obviously, the phase distribution will be changing and should be evaluated. This is not difficult with the above assumption. As shown in Ref.(7), we have

$$\phi = \left[\frac{\dot{\nu}}{2h} t^2 - \frac{E-E_o}{f_o} \left(f \frac{df}{dE} \right) t + \phi_s \right] \cdot 2\pi \ . \qquad (6.1)$$

Eq. (6.1) gives the phase ϕ at the time t of a particle with initial values E and ϕ_s. The conditions for the validity of (6.1) are discussed in Ref.(7), here they are always assumed to be satisfied.

The initial values of the particles were given at an advanced time $\bar{t}$ according to Eq. (6.1). By avoiding the calculation of the energy and the phase for values of $t < \bar{t}$ the computer time was reduced from 10 hours to somewhat more than 1 hour.

7. Description of the data

The computer parameters, λ, Q, ζ, N_h, N_p are listed in Table 4 for the four cases.

TABLE 4

n		λ	Q	ζ	N_h	N_p
0	$\Gamma = 0.50$	3	3	3	160	60(1,2)
	$\Gamma = 0.84$	2	2	2		
10		3	1	30	160	60(1,3)
20		3	1	30	160	60(1,3)
25		6	1	30	160	60(1,-)

The parameter ζ is the number of energy intervals between separatrices contained in the reference channel.

The value $\zeta = 30$ of the cases with $n \neq 0$ was chosen to distribute the particles in an interval between two separatrices bounding one period containing n phase intervals with n suppressed buckets and another period with (h-n) phase intervals and with the (h-n) existing buckets. This was done in order to take into account all the possible trajectories with the same weight.

We took 160 histograms in order to carry out stacking at the top with the last 100 histograms and stacking at the bottom with the first 100 histograms.

The reference channel which initially contained all the particles was the channel No. 80 in which 60 particles were uniformly distributed in energy, having the same synchronous value ϕ_s of the phase of an existing bucket.

The values in brackets in the last column in Table 4 are the numbers of particles eliminated in the subsequent analysis, because they got stuck near to a bucket, in order to make the average change in energy equal to the analytical value. The first number applies to $\Gamma = 0.50$ and the second to $\Gamma = 0.84$.

The parameters describing the RF system are listed in Table 5.

TABLE 5

Γ	0.50	0.84	Units
V	75	1500	Volt
$\dot{\nu}$	-50.0	-1681.9	Hz. V^{-1}
f_o	3.7	13.1	KHz
$f\frac{df}{dE}$	$-4.5.10^{-2}$	$-4.5.10^{-2}$	$eV^{-1}\ s^{-2}$
$2\pi\mathcal{A}$	16	16	eV.s
$\dot{E}_s/E_o$	0.46	16	ms
$\delta E/E_o$	87.10^{-6}	174.10^{-6}	
E_o	300	1000	MeV

where

$\mathcal{A}$ - area of the bucket in the phase space (W,ϕ), with W given by (5.2).
$\dot{E}_s$ - change in time of the energy of synchronous particle.
δE - height of a bucket.

These values, corresponding to moving buckets with Γ and constant, were derived from the Report on the Design Study for the ISR (Ref.[12]), with the exception of the revolution frequency f_o and of the energy E_o at the time $t = 0$ which have been scaled by the same amount according to the considerations made above.

The area of the bucket has been matched roughly to the area that a PS bunch occupies in the (W,ϕ) plane.

It turned out impossible to make calculations for the case $\Gamma = 0.84$ and $n = 25$ because of the high value of Γ and λ. We were not able to understand completely the physical reason of the difficulties encountered but they were certainly related to the high fluctuations involved and the limited number of particles.

8. Phase space trajectories with missing buckets

The value of the phase and of the energy versus time, computed by the ASTACK programme can be plotted in the (E,ϕ) plane each set of initial conditions corresponding to a trajectory of a particle.

They can also be found by an analytical method (see Refs.[9],[10] and [11]).

The results of our plotting are identical to those mentioned in the above references. Figure 2 shows the trajectories in the plane of the scaled variables y, θ for a normal case where $\Gamma = 0.5$ and $h = 3$ (see Ref.[10]). Figure 3 shows the trajectories in the case where the central bucket has been suppressed.

9. Further results from the programme ASTACK

The final value of the energy E_g of the particles, is plotted in Figs. 4, 5, 6, and 7 against the initial value (or the serial number n_p of the particles if they have been numbered from one to the other boundary of the reference channel) for $\Gamma = 0.50$ and $n = 0$, 10, 20, 25 respectively.

Thus the distance in energy between two consecutive separatrices of the trajectories in the (E,ϕ) plane can be found easily. Hence one may judge how well the sample of particles represents all initial conditions with respect to the separatrices.

Whereas Fig. 4 does not require further comments, it should be pointed out that the horizontal full line in Figs. 5, 6 and 7 joins the energies of those particles with initial conditions corresponding to a phase interval with suppressed bucket. The dashed lines correspond to the separatrices as one can easily see from Fig. 4 which may be thought of as an amplification of the energy interval. Each separatrix line connects two particle-points.

The particles on the continuous line have practically not changed the initial energy and the changes occur for the particles having initial energy corresponding to a phase interval occupied by an existing bucket. For these particles we observe a systematical change of the final energy from one particle to the next. This, of course, depends on the choice of the initial value of the energy. This probably indicates how far away a particle is from the next suppressed bucket.

The results for $\Gamma = 0.84$ are, apart from larger fluctuations, not very different from those for $\Gamma = 0.50$.

10. The results from the programme BSTACK

Figures 8, 9, 10 and 11 show some typical histograms for $\Gamma = 0.50$ and $n = 0$, 10, 20, 25 respectively.

The histograms of Fig. 8 should be compared with those obtained by Keil and Nakach (Ref.(8)). There is a good agreement between them. The particles occupied initially the channel No. 80, and the buckets were moving from the left to the right hand side of the figure until they reached the last channel No. 160.

The number given to each histogram is the number of the channel which was being crossed by the buckets(*). Above the channel No. 80, the particles are moved towards the left hand side of the figure decreasing their mean energy.

The situation is quite different for the histograms with $n \neq 0$. The histograms numbered between 1 and 60 do not differ very much. The change occurs from channel No. 80 onwards. Whereas the distribution is steadily decreasing towards the high energy (high value of the channel number) in the

---

(*) The reader should be careful with the notation of our Figs. 8, 9, 10, 11 and that of Ref.(8). The histograms of Keil and Nakach were obtained assuming that the bucket stops in the same channel and that initially the particles are put into different channels. Apart from this difference the distributions in the two cases are exactly the same if one neglects the fluctuations.

case n = 0, a careful analysis of the histograms with n ≠ 0 shows that two distributions are superimposed, the first is equivalent to the case n = 0 and the second one has particles in proximity of channel No. 80 with a spread of a few channels. It is not difficult to recognize in the last distribution those particles which did not change energy during the cycle. The number of these particles increases with n.

From these considerations E. Keil suggested that one could approximate the matrix A by the sum of two particular matrices i.e.:

$$A = \frac{h-n}{h} A_o + \frac{n}{h} U \quad (*) \qquad (10.1)$$

where U is the unit matrix having 1 in the main diagonal, and zeros elsewhere and A_o is the normal matrix for a normal stacking with n = 0.

Inserting (10.1) in (3.1) we have

$$V_{N+1} = \frac{h-n}{h} A_o V_N + \frac{n}{h} V_N + V_B \qquad (10.2)$$

11. The results from the programme CSTACK

11.1 The energy distribution of the stacked beam

The Figs. 12 and 13 show (for $\Gamma = 0.50$) the energy distribution of a stacked beam after N pulses, for stacking at the top and at the bottom respectively and the Figs. 14 and 15 show those for $\Gamma = 0.84$. In these four figures the number of suppressed buckets is n = 10. The cases with other values of n gave similar results.

The curves have been drawn through the points representing the elements of the vector V_N and we averaged the fluctuations which were introduced in our computation.

(*) Since the second superimposed distribution has a spread of a few channels, the matrix U should take into account this spread. But here it is assumed that the spread is contained in channel No. 80.

Our results agree well with those obtained by Keil and Nakach (Ref.[8]).

In the actual energy scale of the ISR, 30 units of horizontal axis correspond to about 8 MeV.

11.2 The stacking efficiency with missing buckets

The stacking efficiency, η was evaluated using the relation (4.1) and has been plotted against the number of pulses $N(n) = N(o) \frac{h}{h-n}$ om Figs. 16 and 17 for stacking at the top and at the bottom at $\Gamma = 0.50$ respectively, and in Figs. 18 and 19 for stacking at the top and at the bottom at $\Gamma = 0.84$ respectively.

Figure 20 shows a comparison of the stacking efficiencies achieved as a function of the ratio n/h for 1500 stacked buckets.

The fundamental result is that, within the statistical error of our calculation, we do not see a variation of the stacking efficiency when the number of suppressed buckets is changed.

12. Acknowledgement

The author wishes to thank Dr. E. Keil for useful discussions, comments and suggestions.

REFERENCES

(1) W. SCHNELL, "Stacking with Missing Buckets, another way of gaining the ISR/PS circumference factor", ISR-RF/66-35 (1966).

(2) W. SCHNELL, "Stacking in Proton Storage Rings with Missing Buckets", Paper presented at the VIth Int. Conf. on High Energy Accelerators, Cambridge 1967.

(3) A.G. RUGGIERO, "Preliminary Studies of the Stacking Efficiency with Missing Buckets", ISR-TH/67-68.

(4) K. HÜBNER, E. JONES, H. KOZIOL, L. MAGNANI, M.J. PENTZ, and A.G. RUGGIERO, "Recent experiments with the CERN Electron Storage and Accumulation Ring (CESAR)", Paper presented at the VIth Int. Conf. on High Energy Accelerators, Cambridge 1967.

(5) E. KEIL, "Stacking in Betatron Phase Space for the ISR", ISR-TH/67-10 (1967).

(6) D.A. SWENSON, "A Study on the Beam Stacking process", Int. Conf. on High Energy Accelerators, Brookhaven (1961), p. 187.

(7) E. KEIL and A.G. RUGGIERO, "Computer method for RF Accelerator Study", CERN, in preparation.

(8) E. KEIL and A. NAKACH, "Beam stacking at high values of $\Gamma = \sin \phi_s$", CERN 66-9, ISR Division, 1966.

(9) K.R. SYMON and A.M. SESSLER, "Methods of Radio Frequency Acceleration in Fixed Field Accelerators with Application to high current and Intersecting Beam Accelerators", CERN Symposium 1956, Part I, p. 44.

(10) N. VOGT-NILSEN, "Theory of RF Acceleration in Fixed Field Circular Accelerators", CERN-PS/NVN-1, (1958).

(11) A.G. RUGGIERO, "A Hamiltonian and phase space trajectories with Missing Buckets", ISR-TH/67-53/Rev. (1967).

(12) ISR Design Study, AR/Int. SG/64-9, 12 May, 1964.

FIGURE CAPTIONS

Fig. 1 — Measured (points) and computed (lines) stacking efficiency in CESAR for 2 cases:
i) 2 full buckets,
ii) 1 full and 1 suppressed bucket.

Fig. 2 — Some trajectories in the (y,θ) plane for the normal case with $\Gamma = 0.5$ and $h = 3$.

Fig. 3 — The same trajectories as modified when the central bucket is suppressed.

Figs. 4,5,6 and 7 — The final energy E_g of the particles placed initially in the channel No. N_r and at the same phase, when they are completely passed by the buckets. On the abscissa the particles are numbered from one boundary to the other of the reference channel (in the sense of increasing energy). $\Gamma = 0.50$.

Figs. 8,9,10 and 11 — Histograms obtained for several values of the number n of suppressed buckets for $\Gamma = 0.5$.
The particles were initially in the channel No. 80.
Each histogram shows the energy distribution at the moment when the bucket crosses the channel with the number indicated. The channel numbers are marked along the abscissa. The ordinate gives the number of particles contained in the channels. The histograms must be read imagining that the bucket moves from the left to the right hand side.

Figs. 12,13,14 and 15 — The energy distributions obtained during the stacking process after N cycles with n = 10. The energy channel numbers are on the abscissa and the density on the ordinate. The distributions are normalized in such a way that an ideal stacking process has a density equal to one. This ideal result is shown by the rectangles.

Figs. 16,17,18 and 19 — The computed stacking efficiency η_N against the number of cycles N and the parameter n.

Fig. 20 — The stacking efficiency η_N against the quantity $\alpha = \frac{h-n}{h}$ after a stacking process for a total of 1,500 stacked buckets.

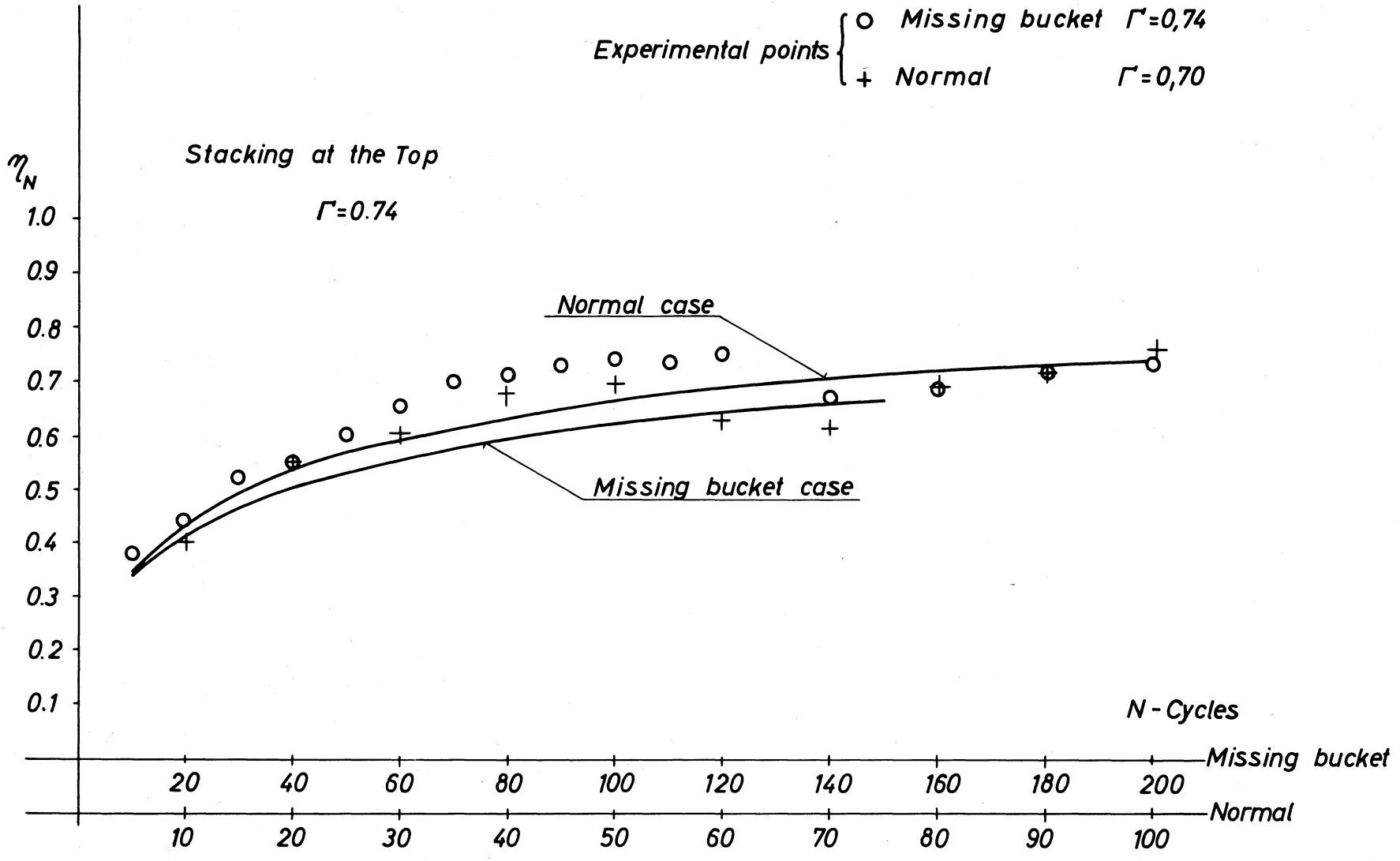
Experimental points
Missing bucket Γ=0,74
Normal Γ=0,70
Stacking at the Top
Γ=0.74
η_N
1.0
0.9
0.8
0.7
0.6
0.5
0.4
0.3
0.2
0.1
Normal case
Missing bucket case
N - Cycles
Missing bucket
20 40 60 80 100 120 140 160 180 200
Normal
10 20 30 40 50 60 70 80 90 100

Fig. 1

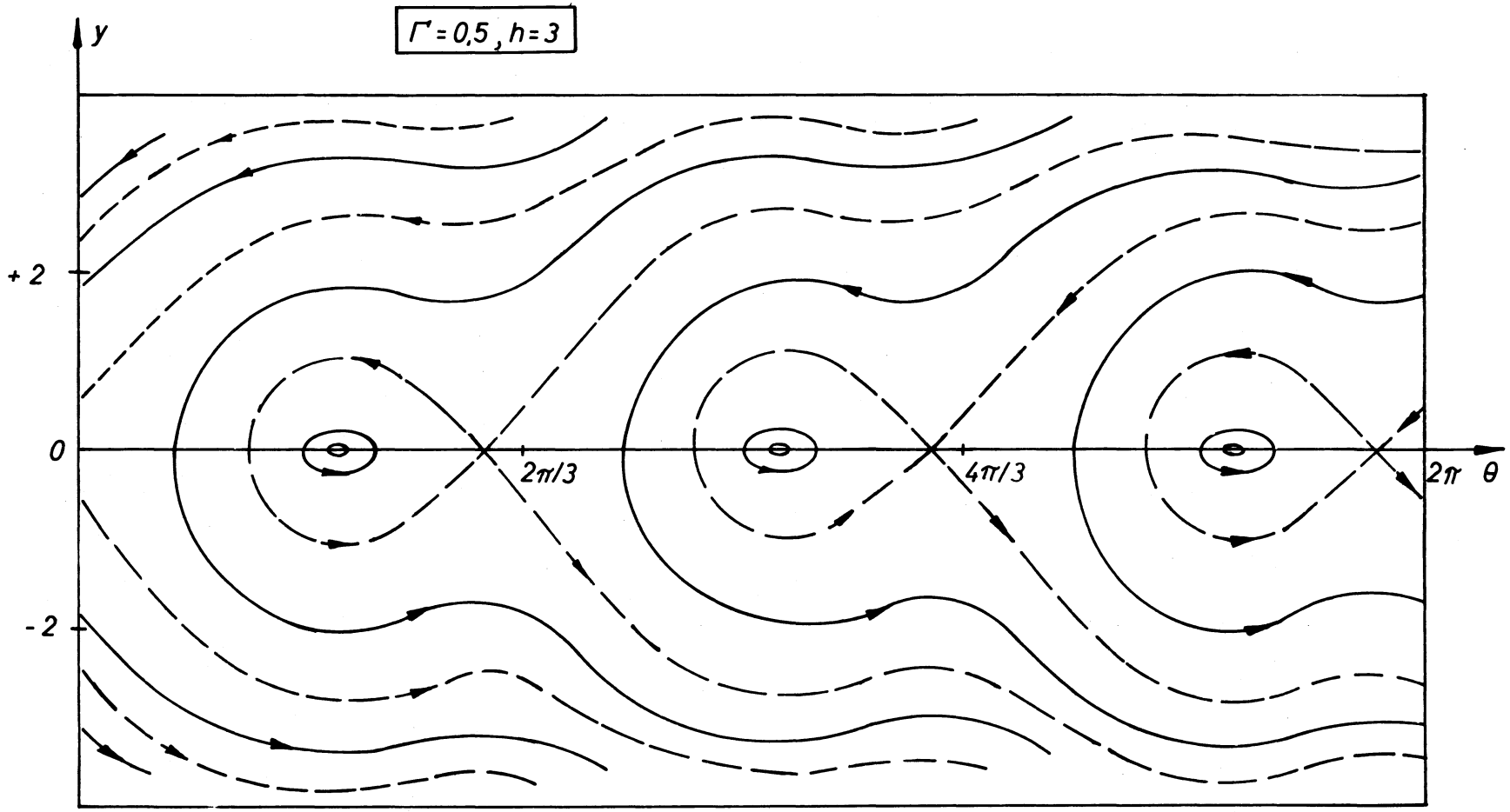

Fig. 2

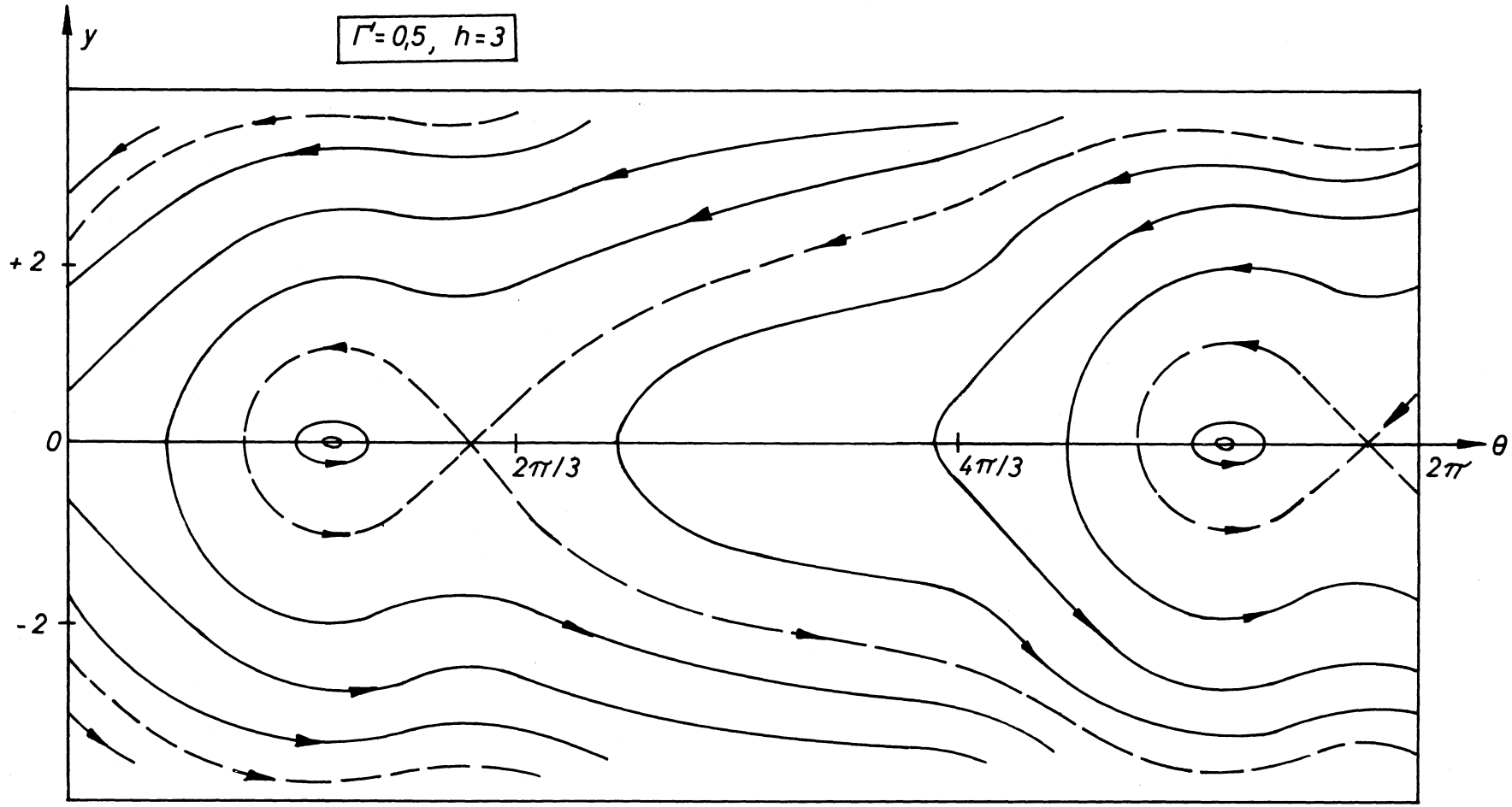

Fig. 3

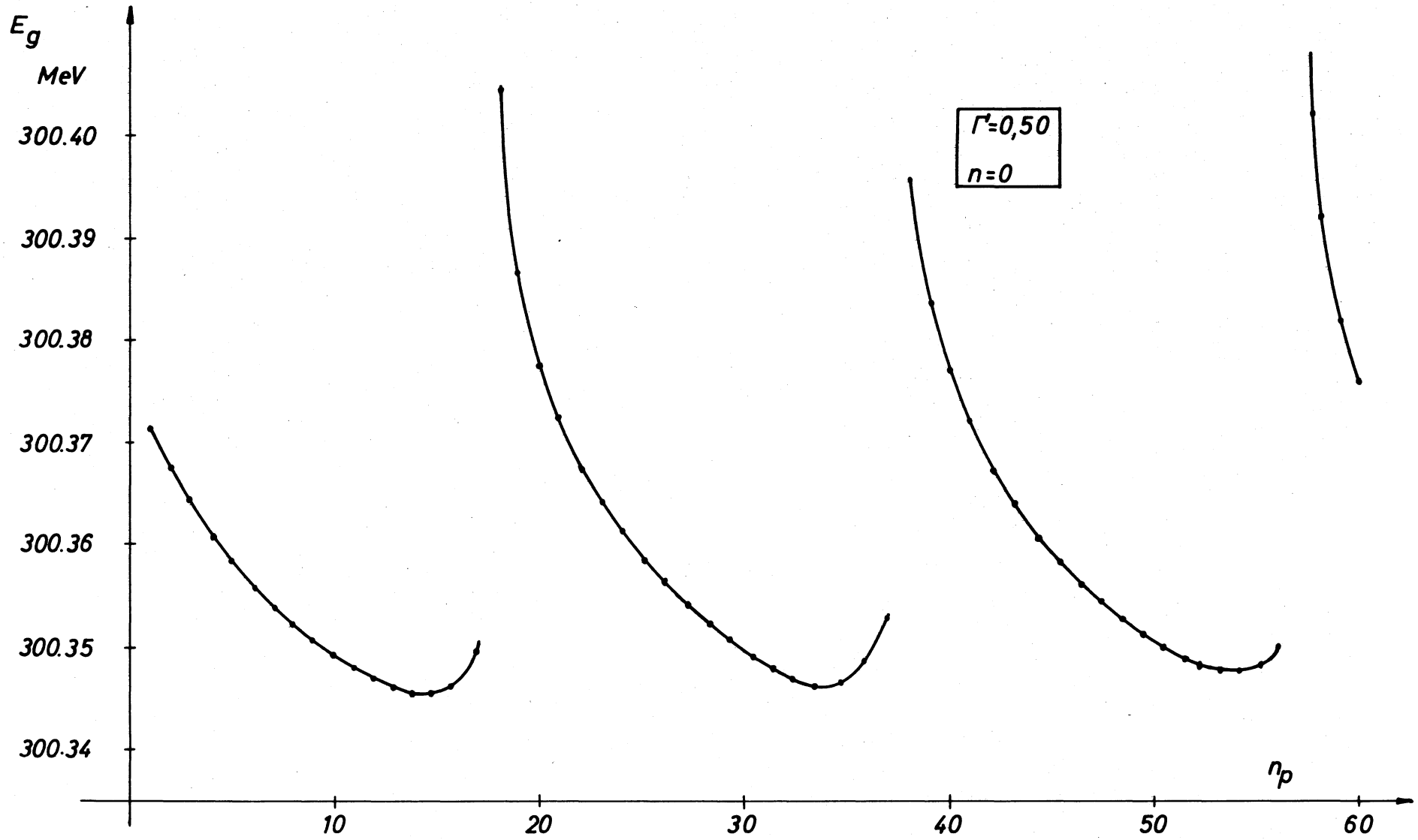
E_g
MeV
300.40
300.39
300.38
300.37
300.36
300.35
300.34
Γ=0,50
n=0
n_p
10
20
30
40
50
60

Fig.4

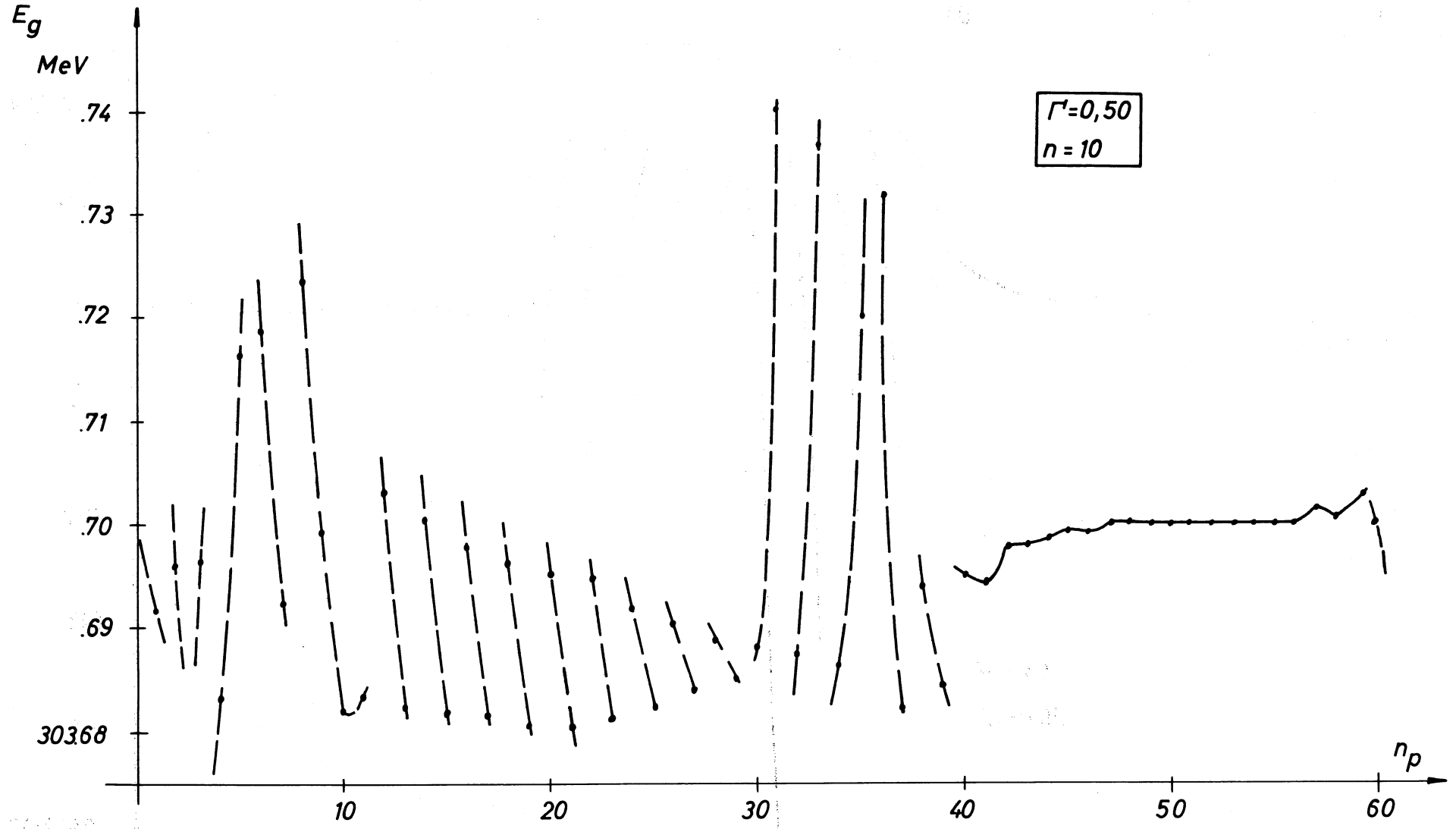

Fig. 5

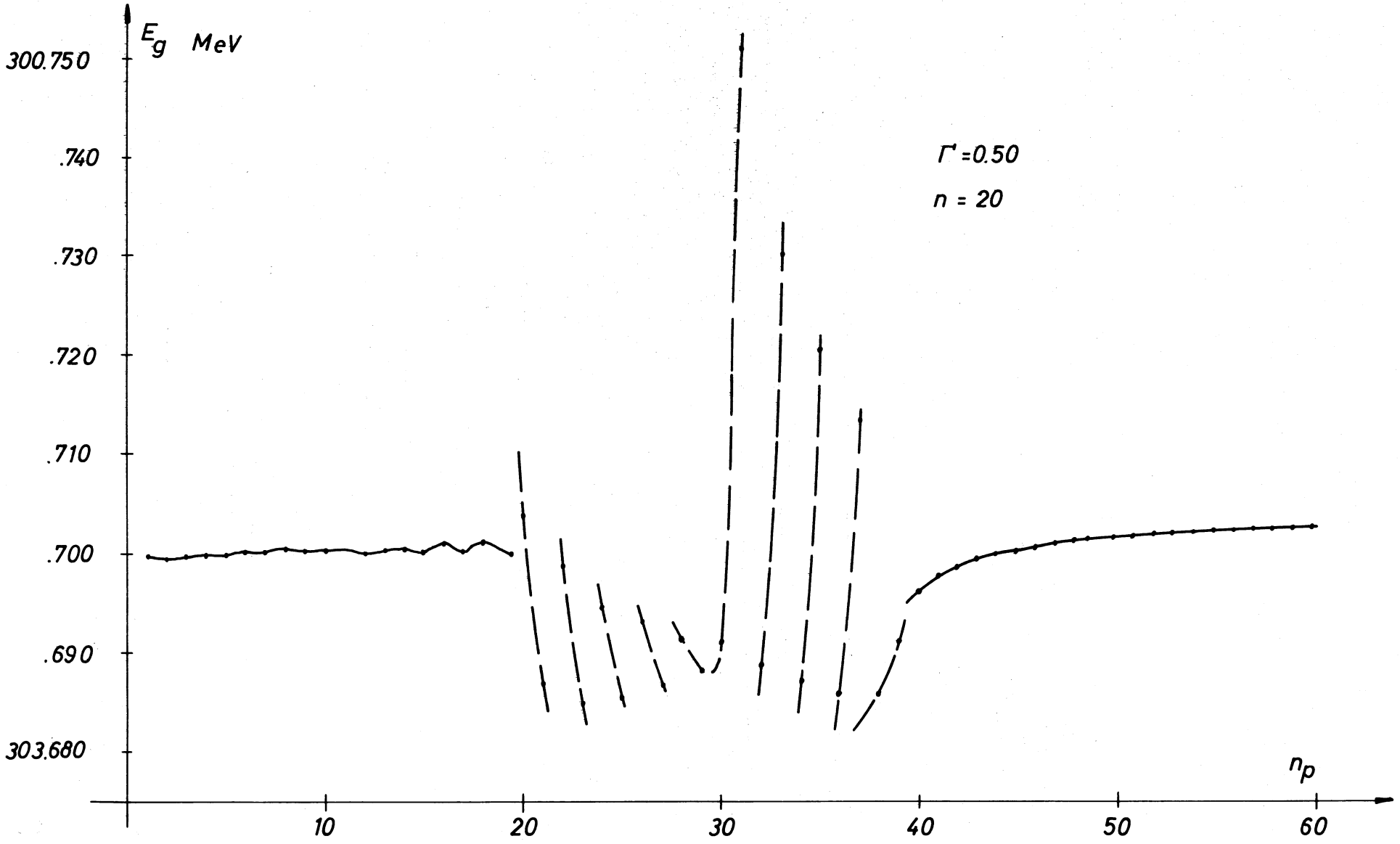
E_g MeV
300.750
.740
.730
.720
.710
.700
.690
303.680
Γ' = 0.50
n = 20
n_p
10
20
30
40
50
60

Fig. 6

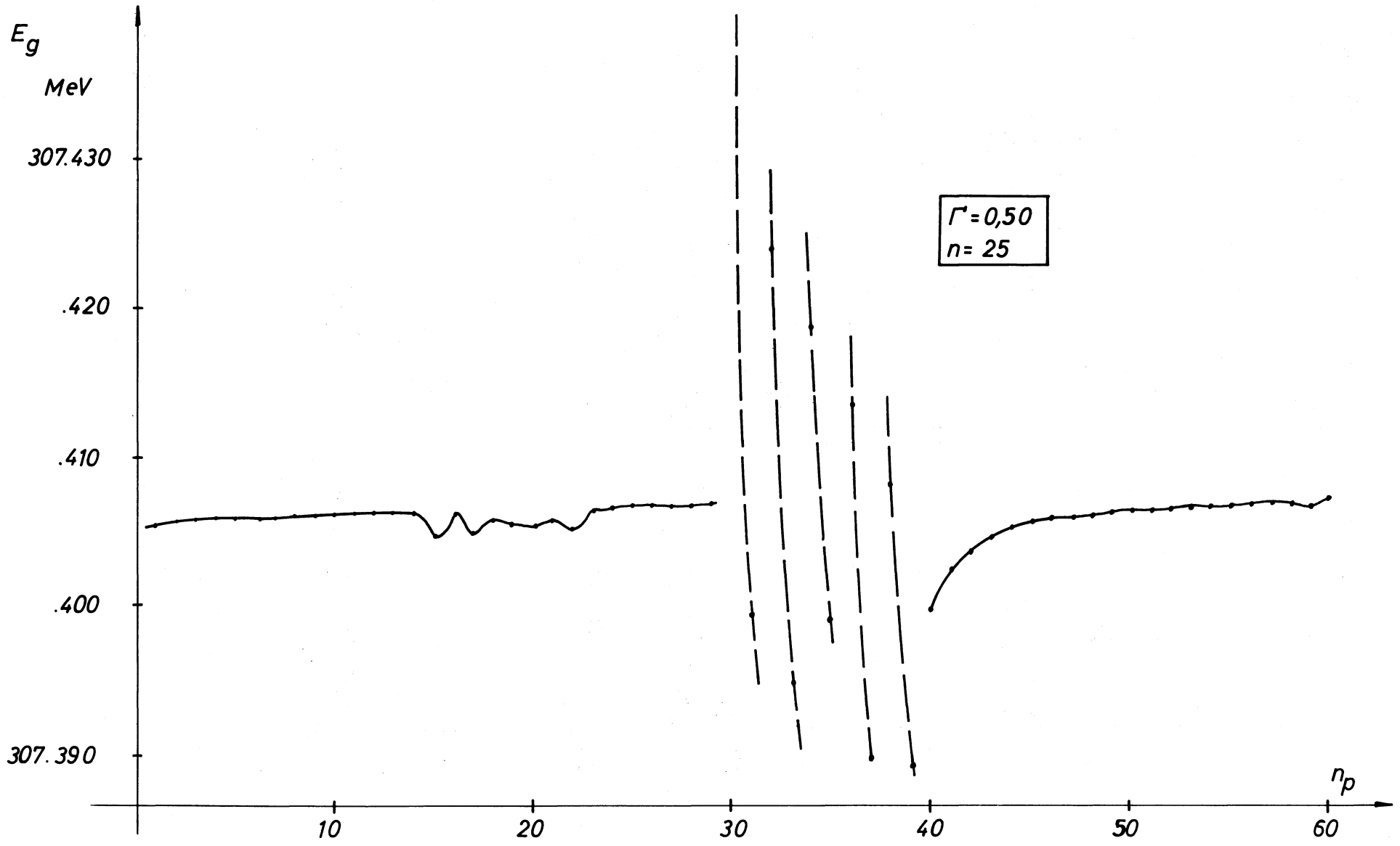
E_g
MeV
307.430
.420
.410
.400
307.390
$\Gamma = 0{,}50$
$n = 25$
10
20
30
40
50
60
n_p

Fig. 7

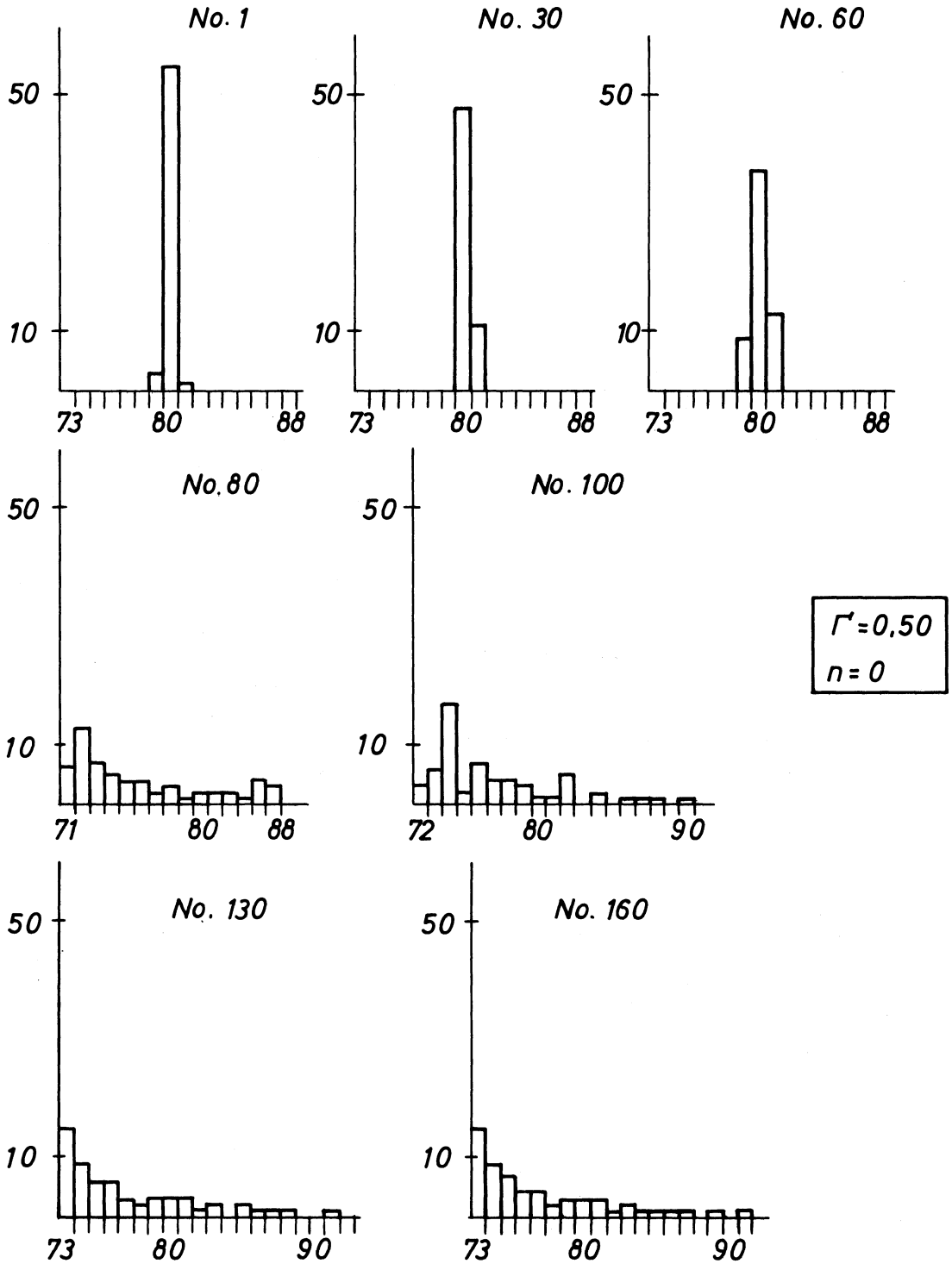
No. 1
No. 30
No. 60
No. 80
No. 100
No. 130
No. 160
50
10
73
80
88
71
72
90
Γ' = 0,50
n = 0

Fig. 8

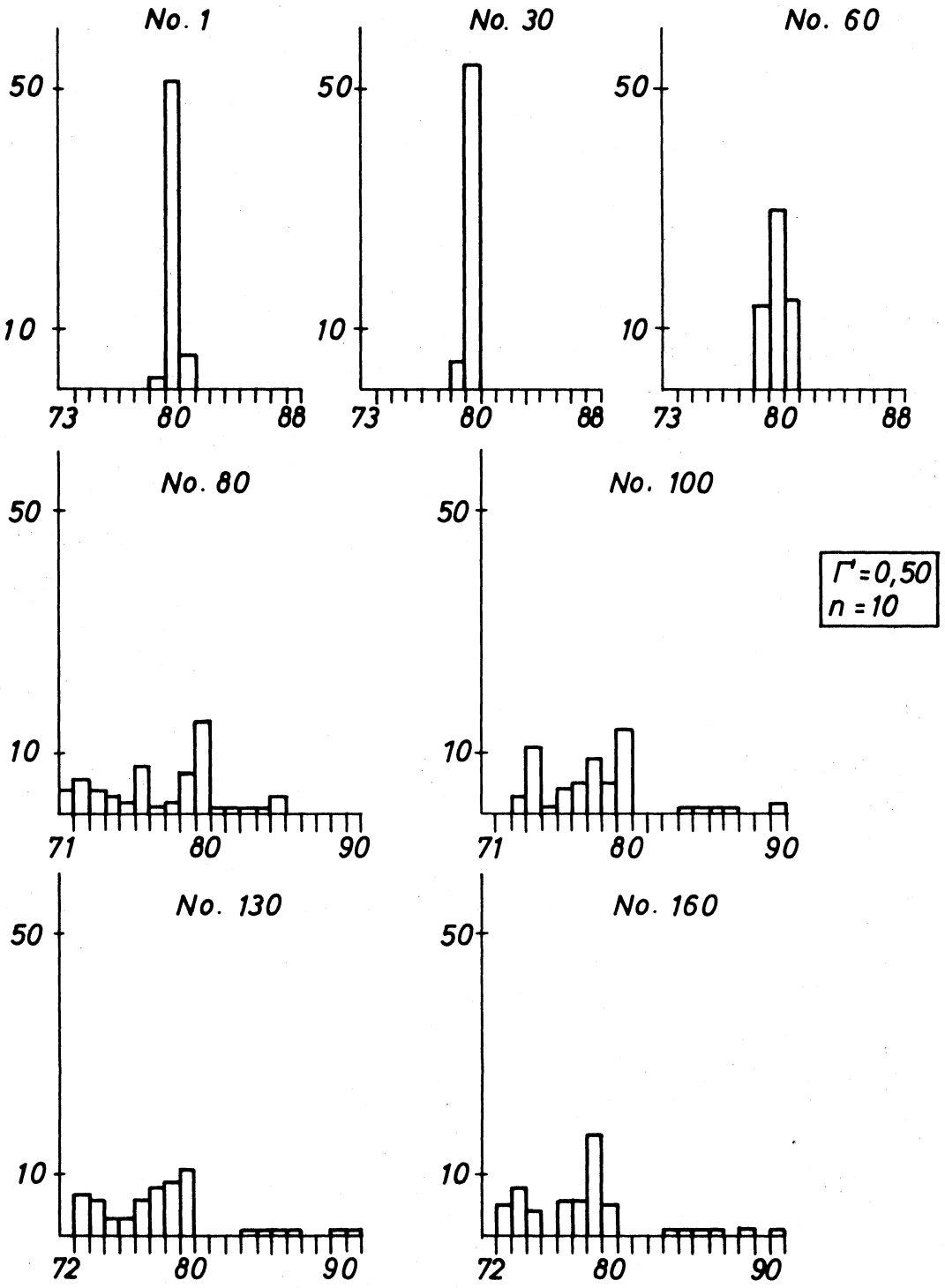
No. 1
No. 30
No. 60
No. 80
No. 100
No. 130
No. 160
50
10
73
80
88
71
90
72
Γ' = 0,50
n = 10

Fig. 9

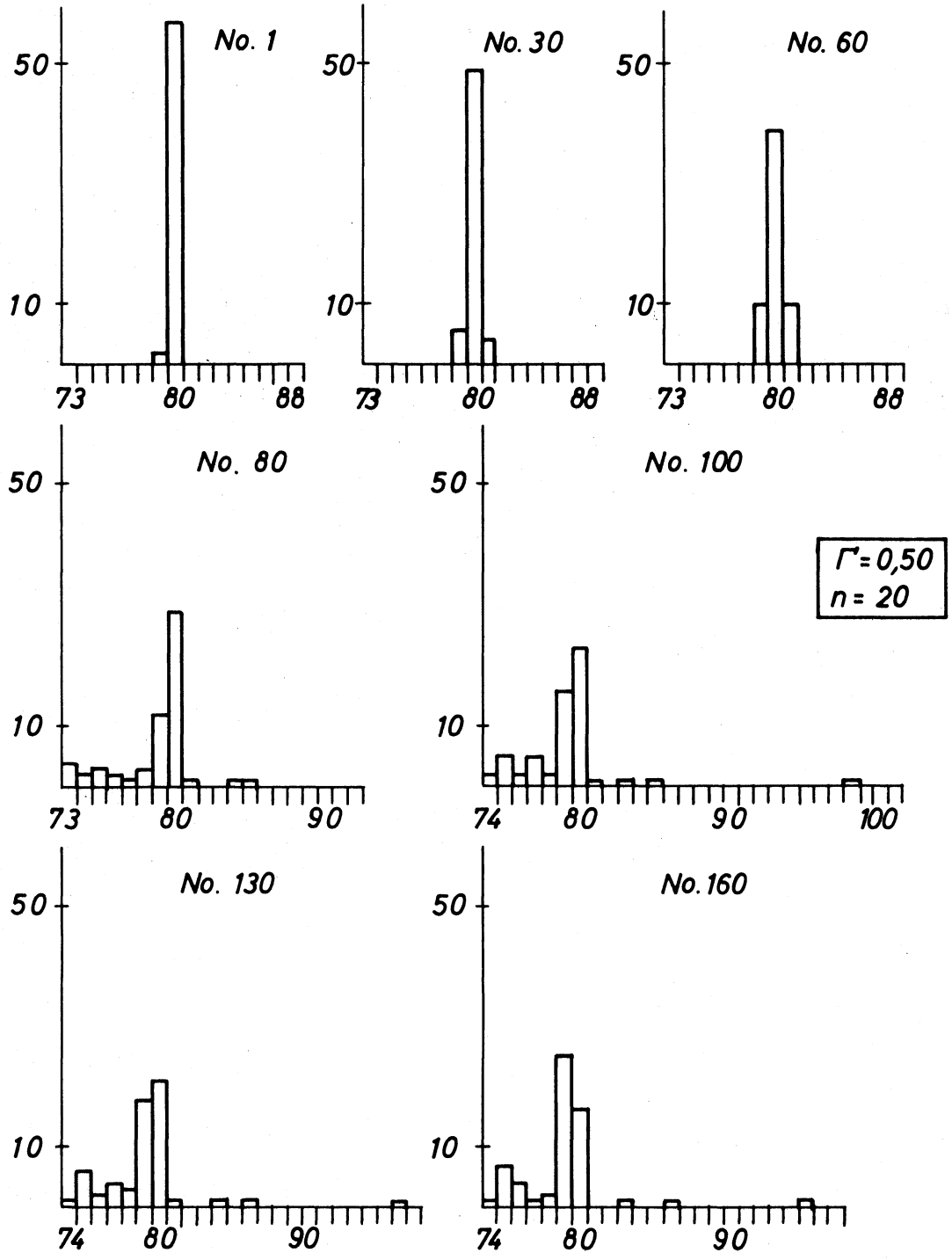
No. 1
No. 30
No. 60
No. 80
No. 100
No. 130
No. 160
50
10
73
80
88
90
74
100
Γ = 0,50
n = 20

Fig. 10

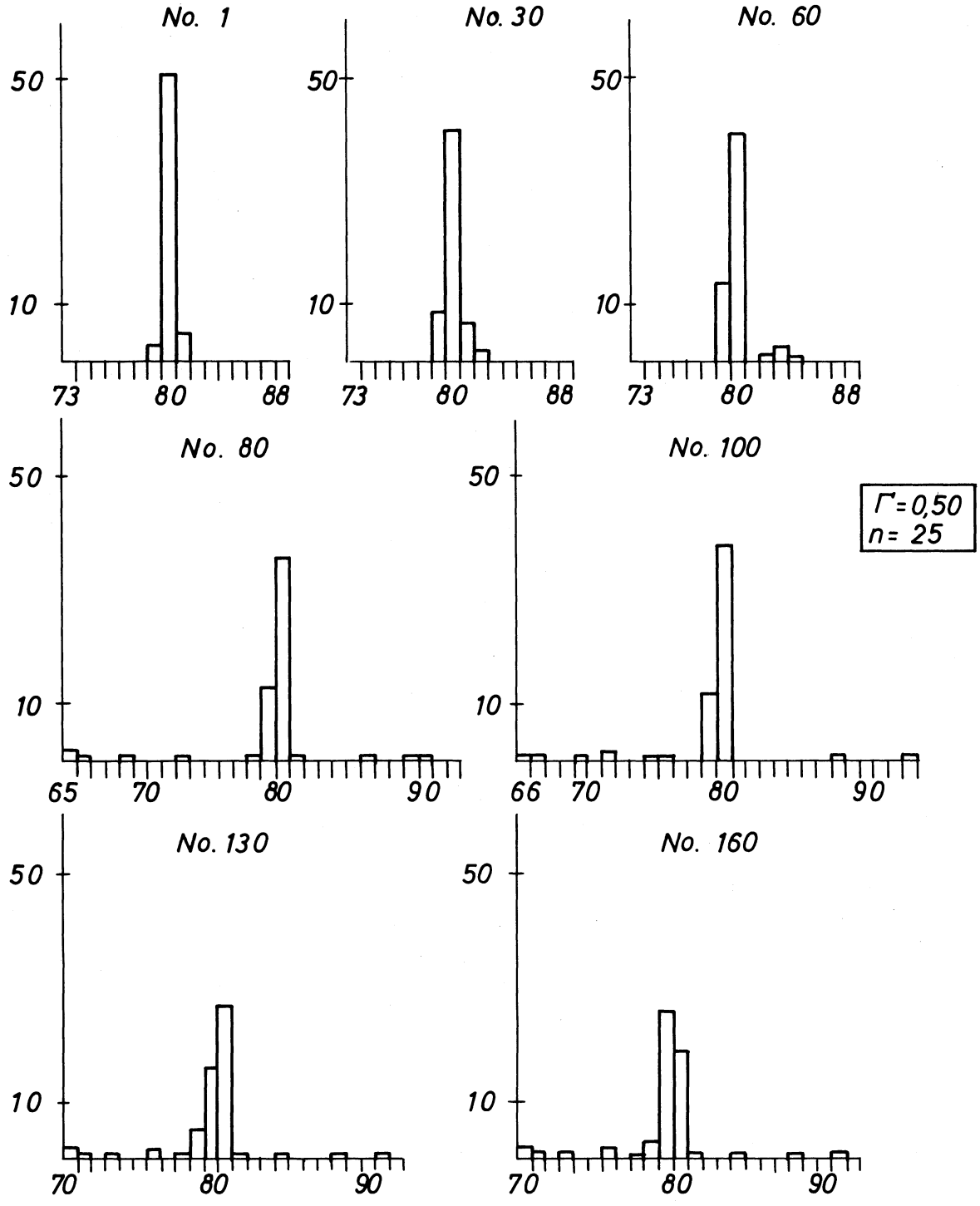
No. 1
No. 30
No. 60
No. 80
No. 100
No. 130
No. 160
50
10
73
80
88
65
70
90
66
Γ = 0,50
n = 25

Fig. 11

Fig. 12 Γ=0,5 Stacking at the top

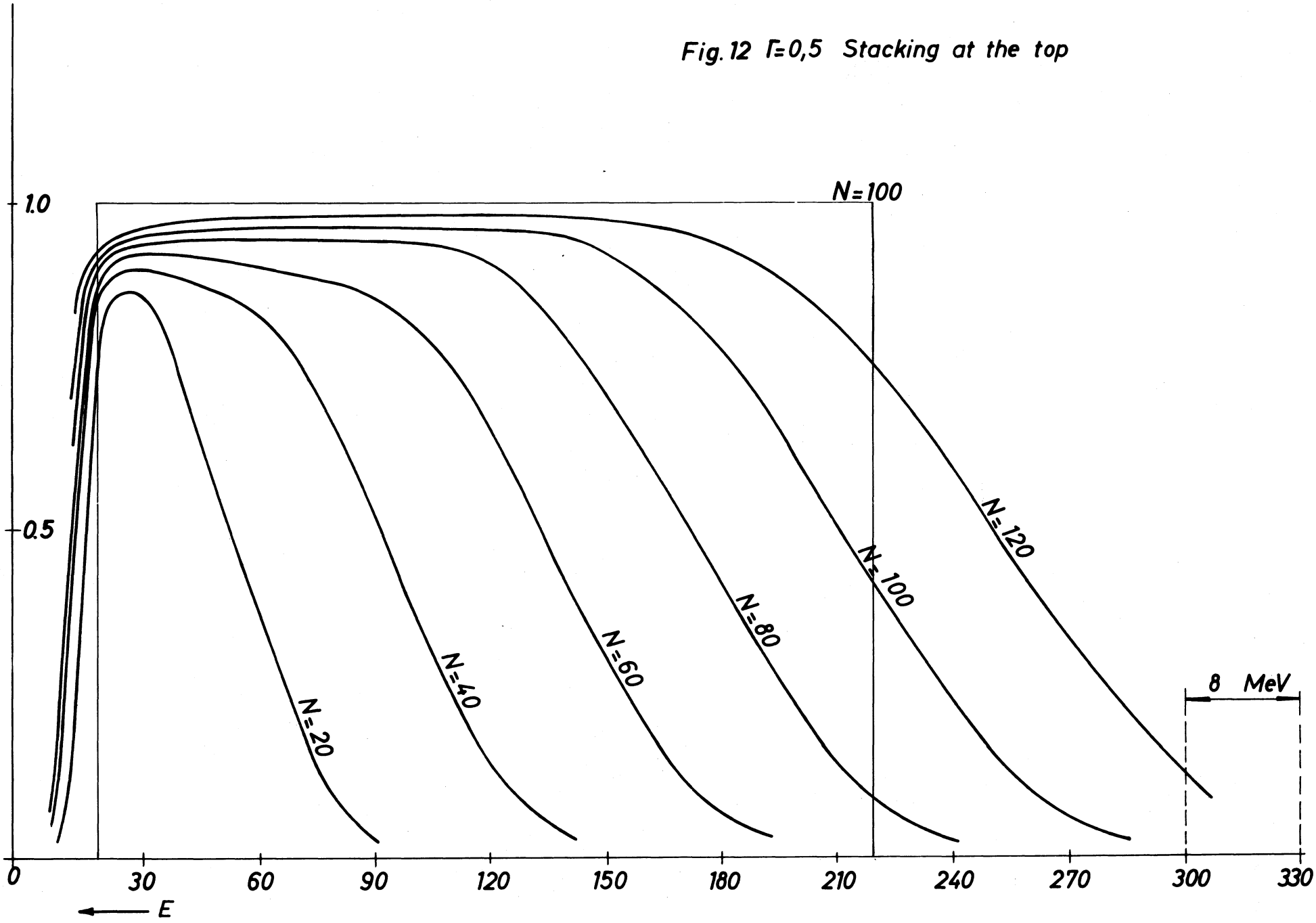

Fig. 13 $\Gamma=0,5$ Stacking at the bottom

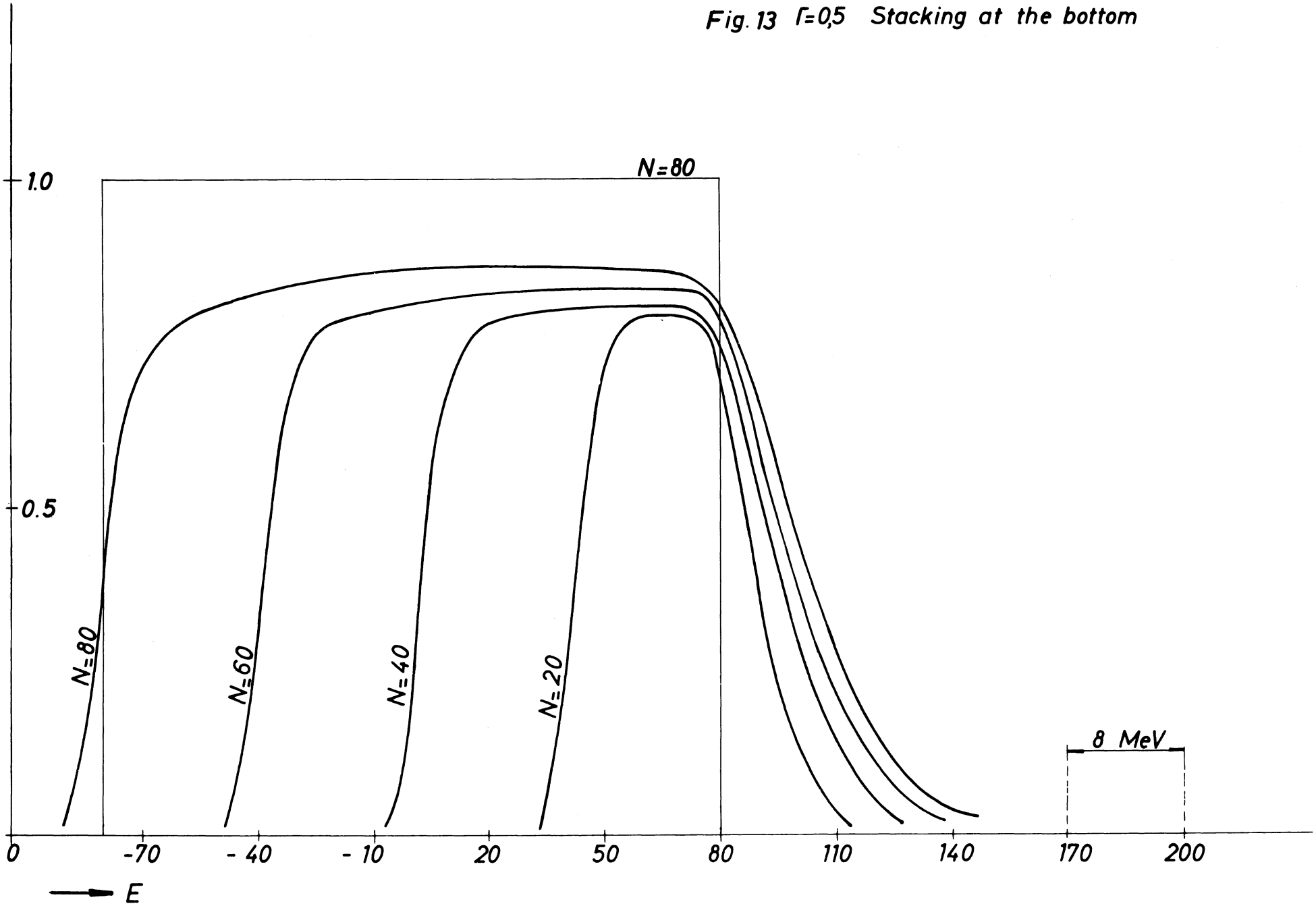

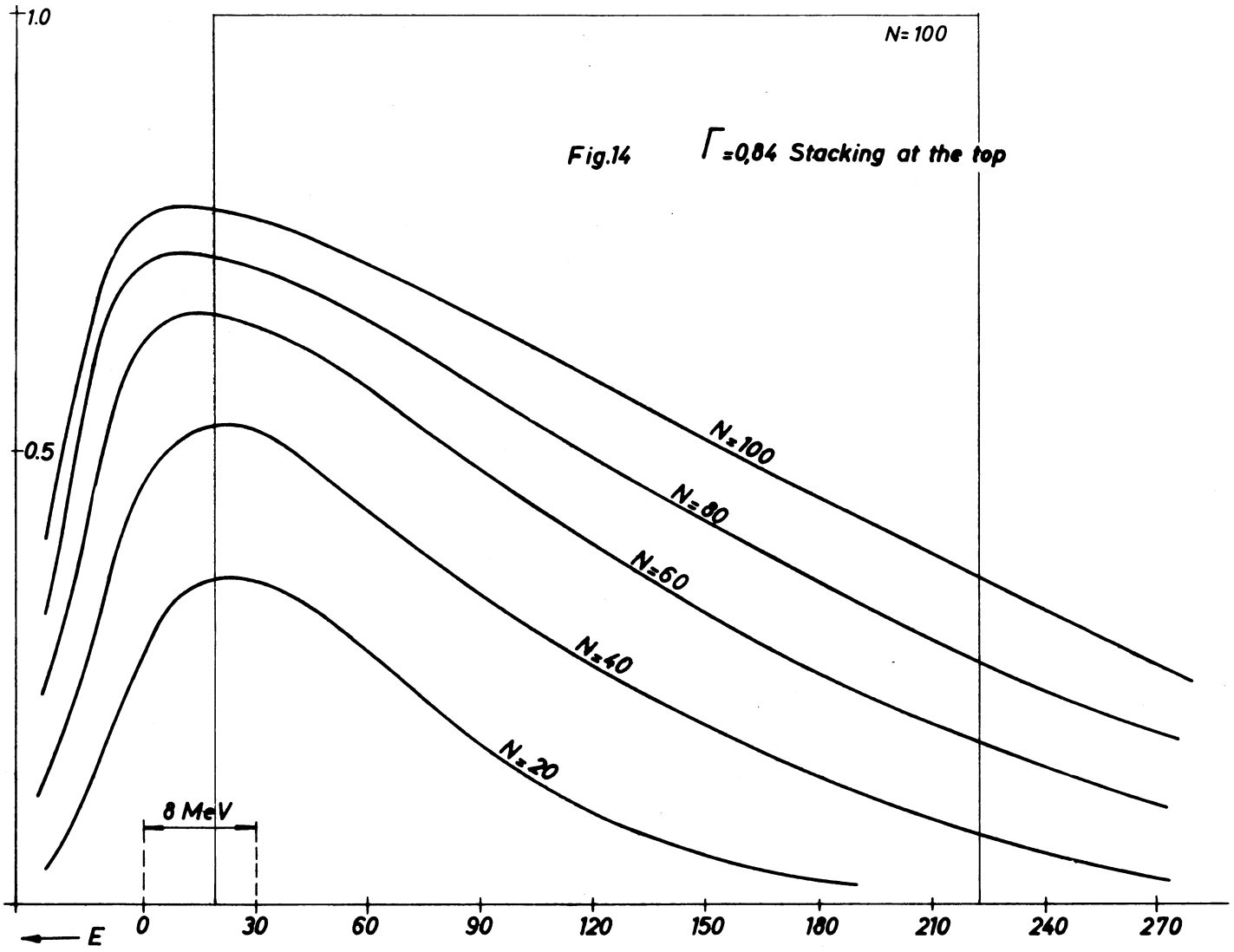

Fig.14 Γ=0,84 Stacking at the top

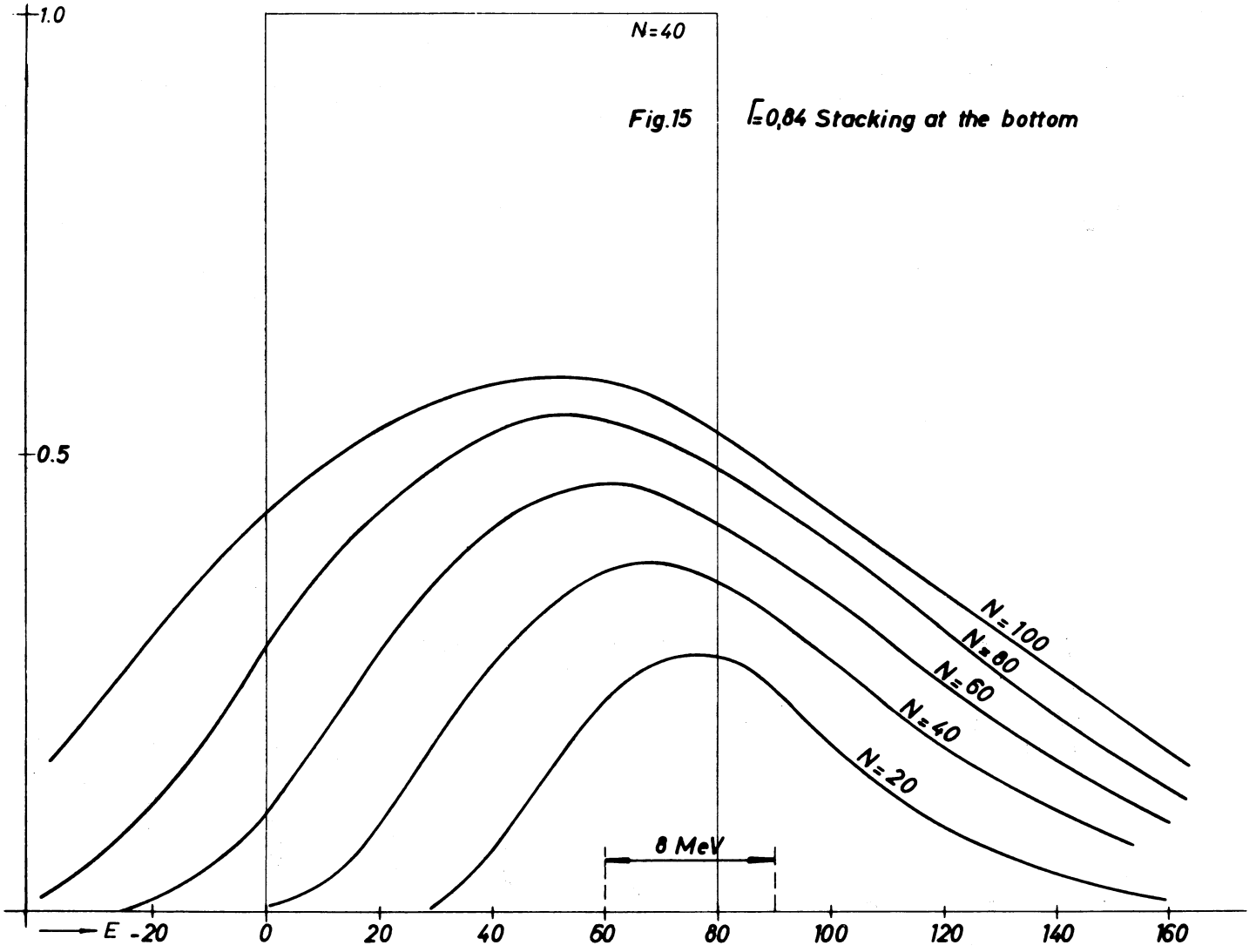
1.0
0.5
N=40
Fig.15
Γ=0,84 Stacking at the bottom
N=100
N=80
N=60
N=40
N=20
8 MeV
E -20
0
20
40
60
80
100
120
140
160

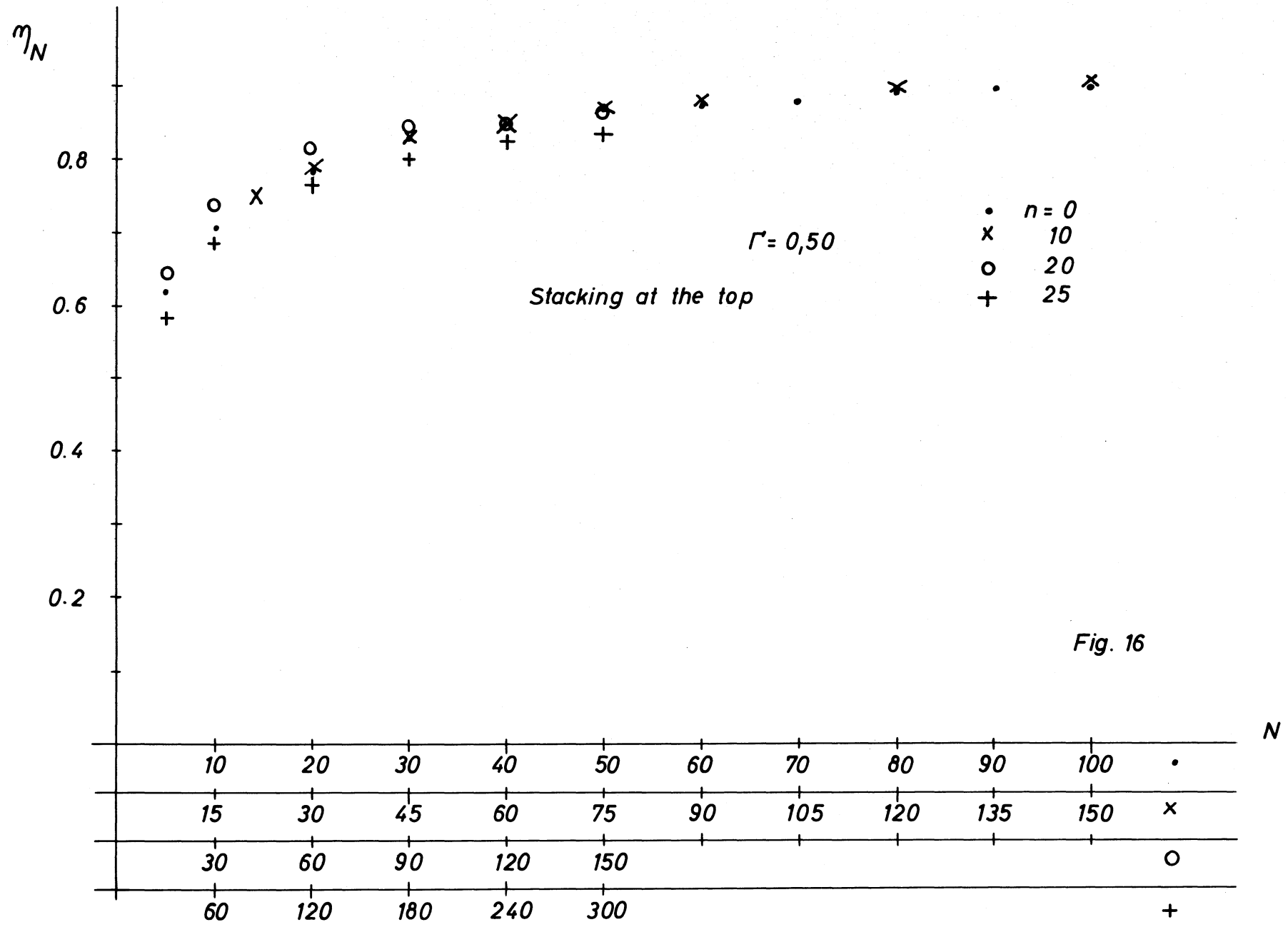
η_N
0.8
0.6
0.4
0.2
$\Gamma = 0{,}50$
Stacking at the top
• n = 0
× 10
○ 20
+ 25
N
10 20 30 40 50 60 70 80 90 100 •
15 30 45 60 75 90 105 120 135 150 ×
30 60 90 120 150 ○
60 120 180 240 300 +

Fig. 16

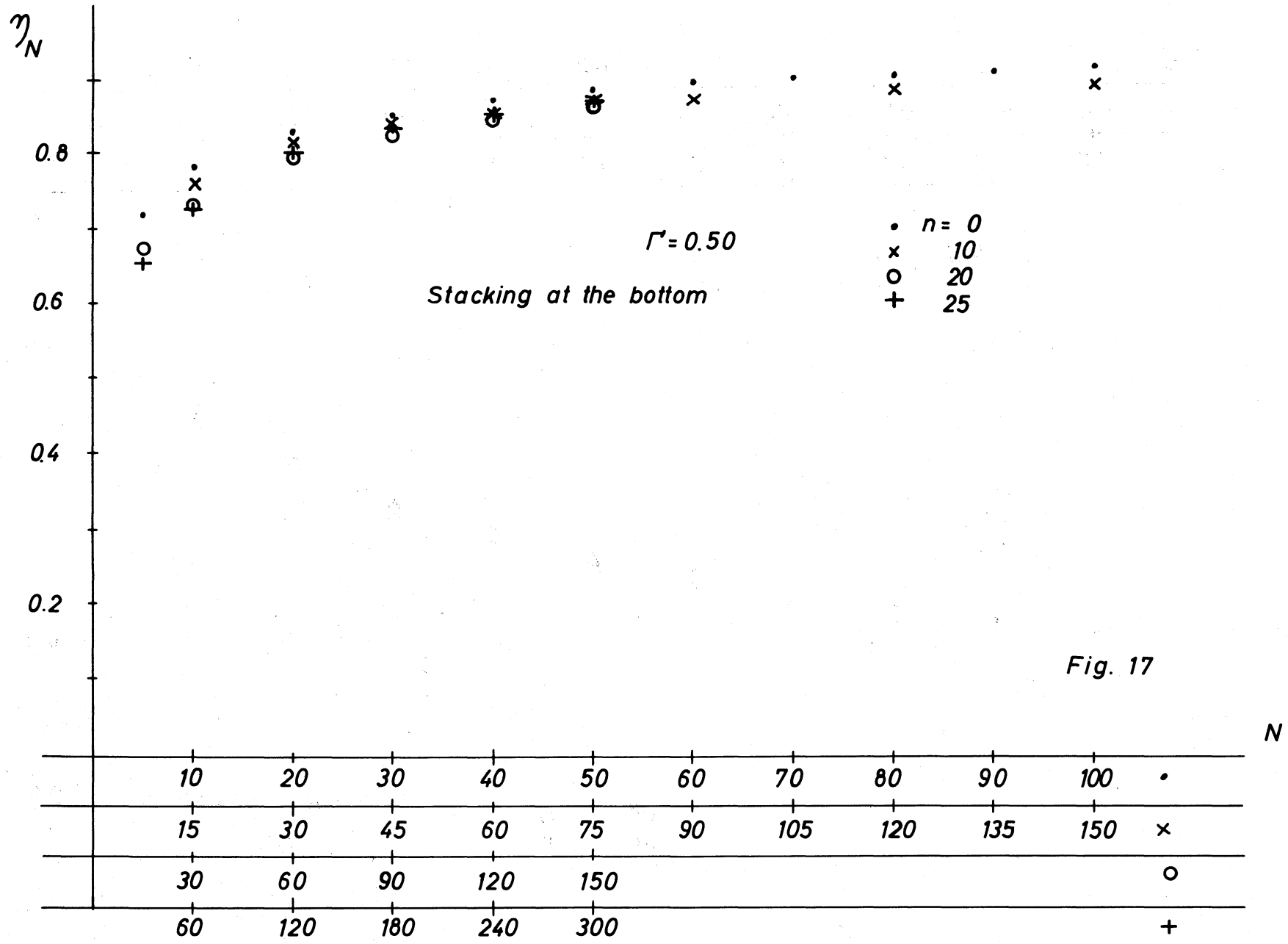
η_N
0.8
0.6
0.4
0.2
$\Gamma' = 0.50$
Stacking at the bottom
• n = 0
× 10
○ 20
+ 25
N
10 20 30 40 50 60 70 80 90 100 •
15 30 45 60 75 90 105 120 135 150 ×
30 60 90 120 150 ○
60 120 180 240 300 +

Fig. 17

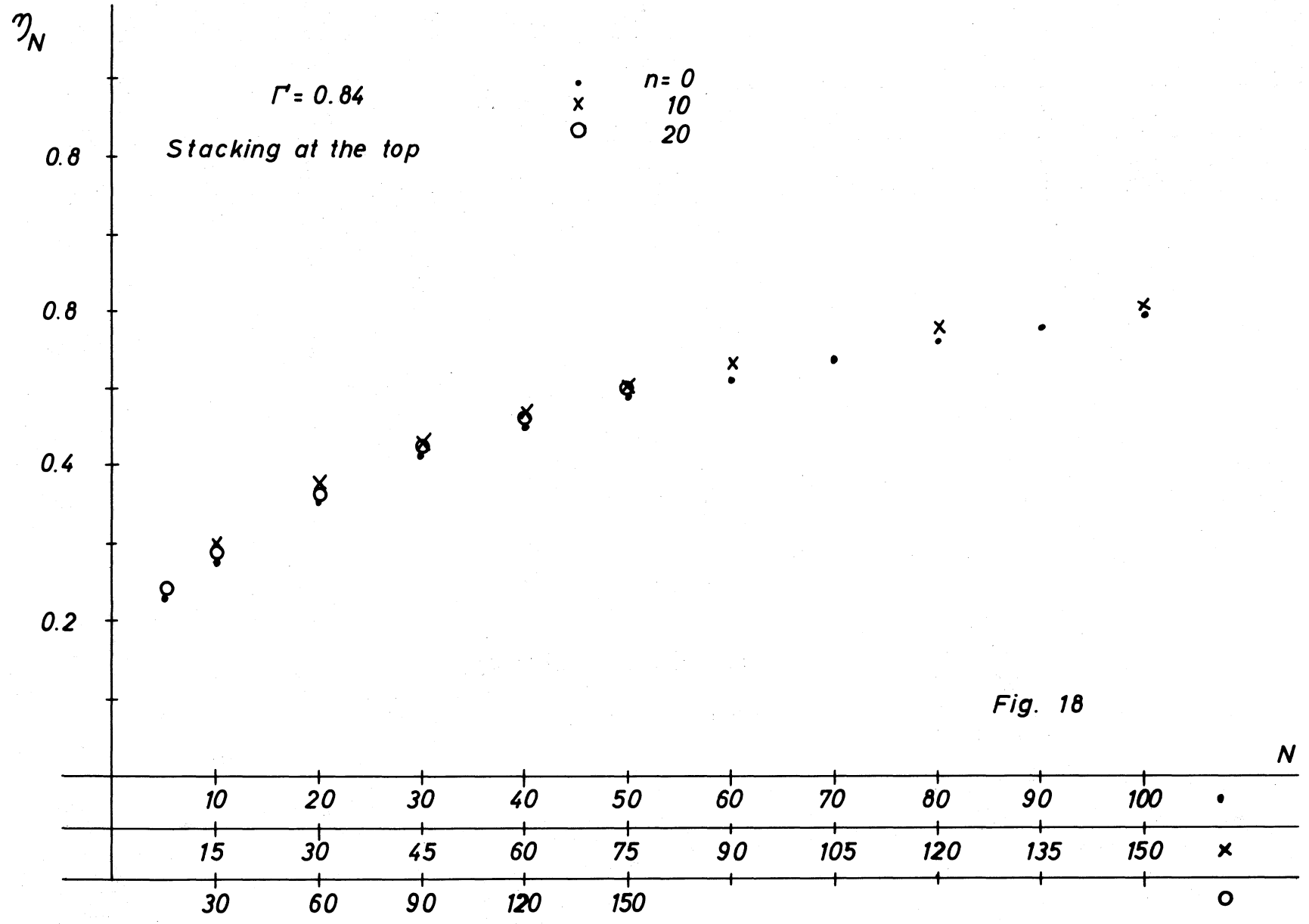
η_N
$\Gamma = 0.84$
Stacking at the top
n= 0
10
20
0.8
0.8
0.4
0.2
N
10 20 30 40 50 60 70 80 90 100
15 30 45 60 75 90 105 120 135 150
30 60 90 120 150

Fig. 18

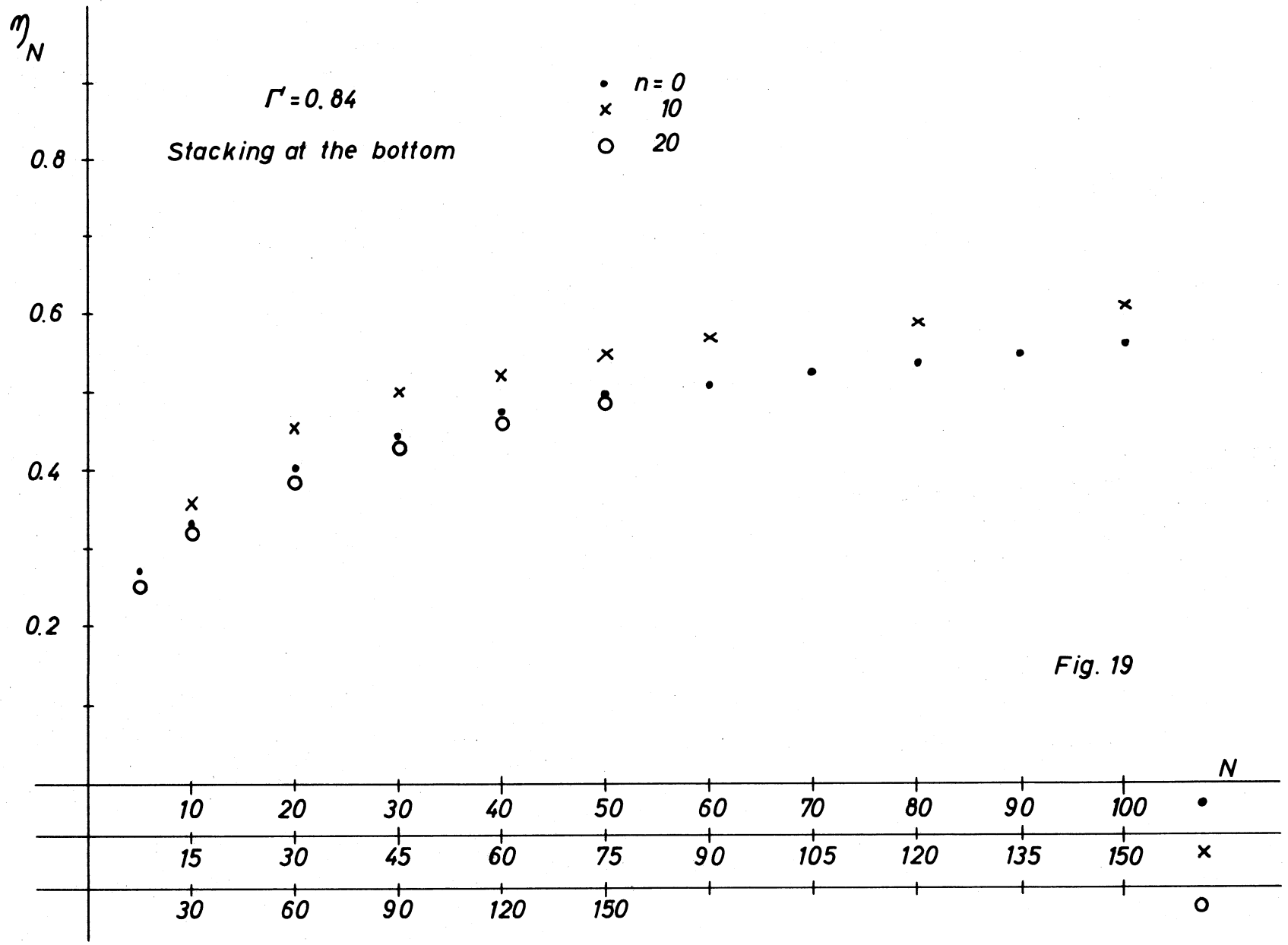
η_N
$\Gamma' = 0.84$
Stacking at the bottom
n = 0
10
20
0.8
0.6
0.4
0.2
N
10 20 30 40 50 60 70 80 90 100
15 30 45 60 75 90 105 120 135 150
30 60 90 120 150

Fig. 19

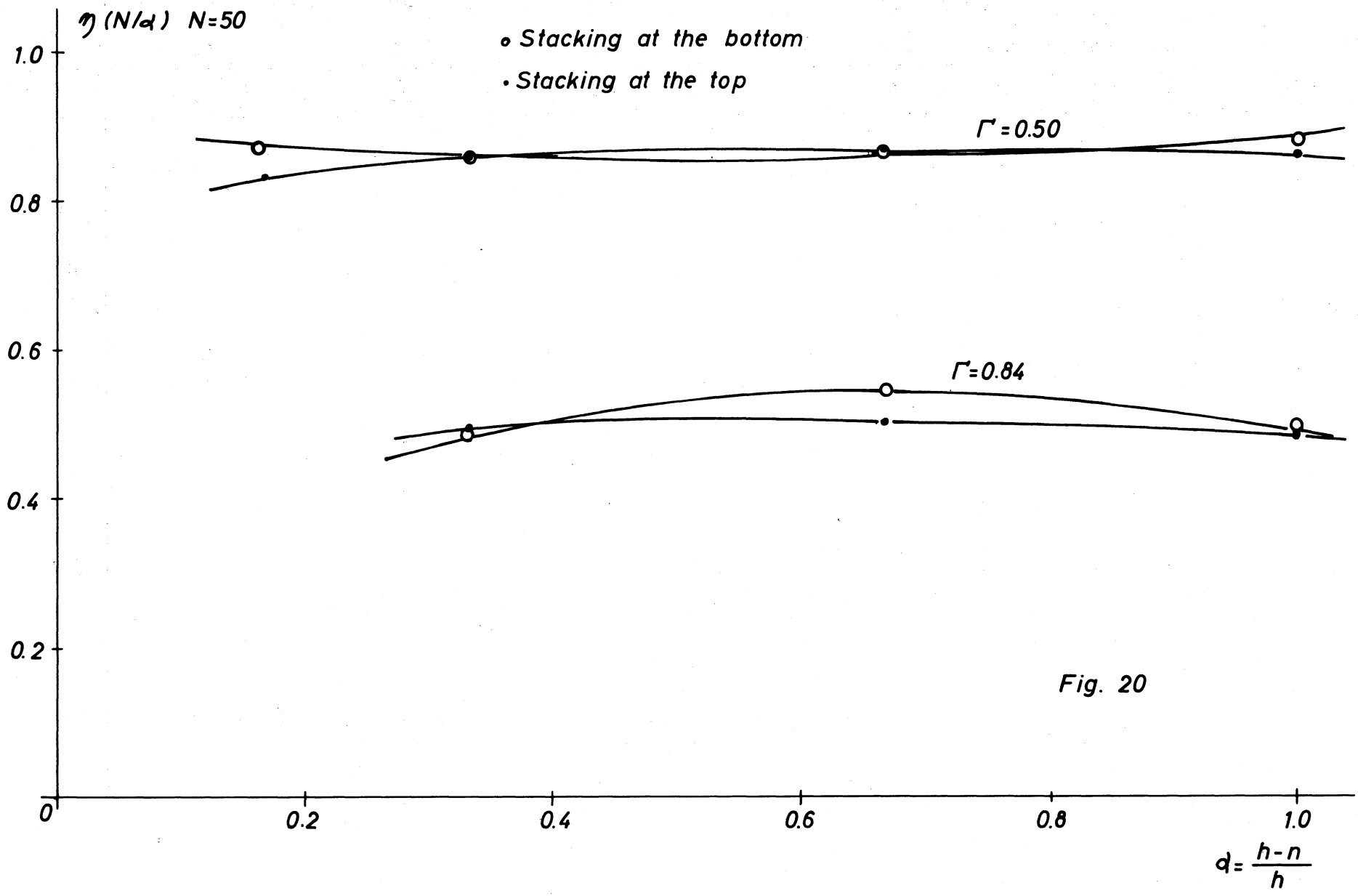
η (N/d) N=50
o Stacking at the bottom
• Stacking at the top
Γ = 0.50
Γ = 0.84
1.0
0.8
0.6
0.4
0.2
0
0.2
0.4
0.6
0.8
1.0
d = h-n/h

Fig. 20